JOURNAL OF GEOPHYSICAL RESEARCH, VOL. 113, D23207, doi:10.1029/2008JD010315, 2008

A study of X-ray emission from laboratory sparks in air at atmospheric pressure

J. R. Dwyer,[1] Z. Saleh,[1] H. K. Rassoul,[1] D. Concha,[1] M. Rahman,[2] V. Cooray,[2] J. Jerauld,[3,4] M. A. Uman,[3] and V. A. Rakov[3]

Received 23 April 2008; revised 17 July 2008; accepted 25 September 2008; published 9 December 2008.

[1] We present a detailed investigation of X-ray emission from long laboratory sparks in air at atmospheric pressure. We studied 231 sparks of both polarities using a 1-MV Marx generator with gap lengths ranging from 10 to 140 cm. The X rays generated by the discharges were measured using five NaI/PMT detectors plus one plastic scintillator/PMT detector, all enclosed in 0.32-cm-thick aluminum boxes. X-ray emission was observed to accompany about 70% of negative polarity sparks and about 10% of positive polarity sparks. For the negative sparks, X-ray emission was observed to occur at two distinct times during the discharge: (1) near the peak voltage, specifically, about 1 μs before the voltage across the gap collapsed, and (2) near the time of the peak current through the gap, during the gap voltage collapse. Using collimators we determined that the former emission emanated from the gap, while the latter appeared to originate from above the gap in the space over the high-voltage components. During individual sparks, the total energy of the X rays that was deposited in a single detector sometimes exceeded 50 MeV, and the maximum energy of individual photons in some cases exceeded 300 keV. X-ray emission near the peak voltage was observed for a wide range of electrode geometries, including 12-cm-diameter spherical electrodes, a result suggesting that the X-ray emission was the result of processes occurring within the air gap and not just due to high electric fields at the electrode.

Citation: Dwyer, J. R., Z. Saleh, H. K. Rassoul, D. Concha, M. Rahman, V. Cooray, J. Jerauld, M. A. Uman, and V. A. Rakov (2008), A study of X-ray emission from laboratory sparks in air at atmospheric pressure, *J. Geophys. Res.*, *113*, D23207, doi:10.1029/2008JD010315.

1. Introduction

[2] X rays have been observed during the dart leader phase of rocket-triggered and natural cloud-to-ground lightning, during the formation of the steps in the stepped leader phase of natural lightning, and from ground-based and in situ measurements during thunderstorms [*Moore et al.*, 2001; *Dwyer et al.*, 2003, 2004a, 2005b]. In addition, gamma rays with energies up to 20 MeV have also been observed by spacecraft to emanate from the atmosphere [*Fishman et al.*, 1994; *Smith et al.*, 2005; *Dwyer and Smith*, 2005] and have been observed from the thundercloud in the initial stage of one triggered lightning flash [*Dwyer et al.*, 2004b]. The mechanisms for producing such X rays and gamma rays are presently under active debate, but they almost certainly involve the acceleration of high-energy electrons, known as runaway electrons, under the influence of strong electric fields in air [*Gurevich and Zybin*, 2001].

[3] When the rate of energy gain from the electric field experienced by an electron moving through air exceeds the rate of energy loss, caused predominantly by ionization energy losses, then the electron will gain energy [*Wilson*, 1925]. This is illustrated in Figure 1, which shows the rate of energy loss experienced by an electron moving through air at standard conditions [*Dwyer*, 2004]. As can be seen, the rate of energy loss peaks at the kinetic energy about 100 eV and then decreases with increasing energy. As a result, for sufficiently strong electric fields, it is possible for electrons with energies over 100 eV to run away, gaining very large energies from the electric field. In particular, if the electric field exceeds the critical field, $E_c \sim 30$ MV/m, about 10 times the field needed for conventional breakdown, then the tail of the "thermal" electron population can exceed 100 eV, allowing these electrons to run away. In other words, the seed electrons that run away come from the ionization of the gas, for example, at streamer tips. This is the so-called cold runaway breakdown mechanism [*Gurevich*, 1961], which does not require an external source of energetic seed particles. As the energetic electrons move through air, or when they strike an electrode they will emit bremsstrahlung (braking) radiation in the form of X rays,

[1]Department of Physics and Space Sciences, Florida Institute of Technology, Melbourne, Florida, USA.
[2]Ångström Laboratory, Division for Electricity and Lightning Research, Department of Engineering Sciences, Uppsala University, Uppsala, Sweden.
[3]Department of Electrical and Computer Engineering, University of Florida, Gainesville, Florida, USA.
[4]Now at Raytheon Missile Systems, Tucson, Arizona, USA.

0148-0227/08/2008JD010315$09.00

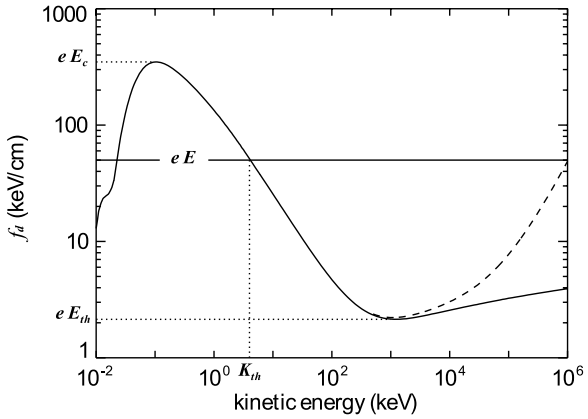

Figure 1. Rate of energy loss experienced by a free electron moving through air at STP as a function of kinetic energy [from *Dwyer*, 2004]. The solid curve is due to inelastic scattering of the electron with air molecules, and the dashed curve includes the effects of bremsstrahlung emission. The horizontal line shows the electric force from a 5 MV/m electric field. Runaway electrons occur for kinetic energies greater than the threshold energy, $K > K_{th}$. E_c is the critical electric field strength for which part of the low-energy electron population will run away, and E_{th} is the minimum field needed to produce relativistic runaway electrons.

with energies extending up to the energy of the incident electrons. *Dwyer* [2004] suggested that cold-runaway breakdown, possibly from the streamer (cold discharge) tips or from the leader (hot conducting channel), could explain the X-ray emission observed from lightning. *Moss et al.* [2006] performed Monte Carlo simulations to show that, in some circumstances, the streamers could produce cold runaway electrons.

[4] An alternative possibility for producing runaway electrons is the Relativistic Runaway Electron Avalanche (RREA) mechanism [*Gurevich et al.*, 1992; *Lehtinen et al.*, 1999]. As can be seen in Figure 1, even for electric fields with $E < E_c$, electrons can run away as long as their initial kinetic energy is greater than the threshold energy, K_{th}. These electrons can, in turn, create more energetic electrons above the threshold energy via hard elastic scattering with atomic electrons, resulting in an avalanche of relativistic electrons. In other words, ionization and the subsequent acceleration of electrons, followed by more ionization and acceleration results in an avalanche of runaway electrons. This mechanism requires the electric field to exceed the avalanche threshold ($E_{th} \sim 0.28$ MV/m) over a distance of several hundreds of meters [*Coleman and Dwyer*, 2006]. The energetic seed electrons that initiate the avalanches can be supplied by atmospheric cosmic rays, and, in some cases, by a feedback effect mediated by backward propagating positrons and backward scattered X rays [*Dwyer*, 2003]. This latter mechanism is called relativistic feedback and can generate very large quantities of runaway electrons and X rays [*Dwyer*, 2007]. However, for both RREA acting on external seed particles and the relativistic feedback mechanism, the potential difference needed to produce substantial numbers of runaway electrons is several tens of MV. Although such potential differences cannot be ruled out in the case of lightning, they can be ruled out for the case of laboratory sparks where the potential difference is known. As a result, since there currently is not a viable alternative, the observation of X-ray emission from laboratory sparks lends strong support to the cold runaway electron mechanism and indicates that at some location within the air gap electric fields in excess of E_c are present.

[5] The experimental search for X-ray emission from laboratory sparks at various pressures has a long history [*Noggle et al.*, 1968; *Stankevich and Kalinin*, 1968; *Tarasova and Khudyakova*, 1970; *Tarasova et al.*, 1974; *Babich et al.*, 1975]. Some investigators have studied the production of X rays in small ($\sim$1 mm) gaps at low pressures (<1 torr) with very large over-voltages [e.g., *Va'vra et al.*, 1998]. Such X-ray emission is not surprising given the behavior of the Paschen curve at low gas densities [*Brown*, 1966]. For small gap lengths and low pressures, according to the Paschen curve, the dielectric breakdown field no longer obeys the scaling law, $E_b \propto n$, and the reduced dielectric breakdown field, E_b/n, increases with decreasing density, n. For an air gap length of 1 mm, for example, the dielectric breakdown field actually exceeds the critical field, E_c, for densities below about 10 torr, owing to the long mean-free-paths of the electrons at this low density. As a result, electrons will gain large energies when traversing the gap, owing to the low number of collisions with the gas molecules, and X rays will be produced when they strike the anode. One way to think about this is that, as the air is evacuated, the discharge gap starts acting like a standard X-ray tube. It follows that these experiments probably have little to do with the production of X rays by thunderstorms, lightning, or long laboratory sparks at atmospheric pressure.

[6] On the other hand, for sparks in air at 1 atmosphere pressure, the dielectric breakdown field in a uniform gap, E_b, is $\sim$3 MV/m, which, as noted earlier, is a factor of 10 below the critical field, E_c, of $\sim$30 MV/m. Furthermore, the average electric field in a long gap can be a factor of ten or more below E_b. Consequently, without the insight given by the X-ray observations, there is little a priori reason to suppose that the critical field is ever reached during such discharges. It follows that, if such critical fields are produced, they must occur through the complex action of large numbers of electrons (space charge), such as near the tips of streamers or near the leader channel.

[7] Motivated by the X-ray observations of natural and triggered lightning, *Dwyer et al.* [2005a] performed X-ray observations of long laboratory sparks in air using a 1.5 MV Marx generator. These experiments are briefly described here: X-ray observations were made during fourteen 1.5- to 2.0-m-long discharges in air. All 14 discharges generated X rays in the $\sim$30 to 150 keV range. The X rays, which arrived in discrete bursts, less than 0.5 μs in duration, occurred from both positive and negative polarity rod-to-plane discharges as well as from small, 5–10 cm, series spark gaps within the Marx generator. For the positive spark measurements, the X-ray bursts occurred prior to the main high-current arc, at a time when the electric fields in both small and large gaps were near their maximum. The same was generally true for the negative sparks, with the exception of three sparks that also produced X rays while the voltage across the main gap was collapsing.

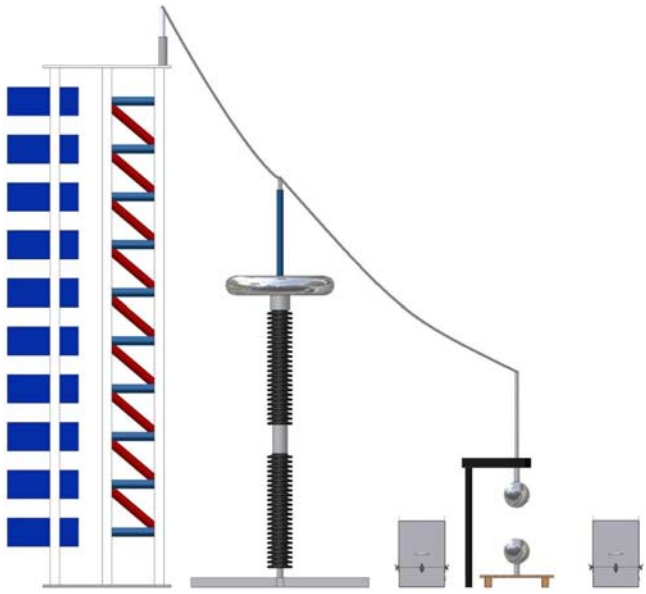

Figure 2. Schematic of experimental setup, showing the approximate arrangement (from left to right) of the Marx generator, HV divider, spark gap (shown in vertical configuration) and two of the three X-ray instruments. The components are only approximately to scale and the image is meant only to illustrate the relative placements. For reference, the X-ray instruments measure 50 cm on a side.

[8] It is not immediately obvious what properties of the Marx generator used by *Dwyer et al.* [2005a] are important for the production of X rays by sparks. We consider three properties here: (1) The Marx generator produced very large current pulses, measured in kilo-amperes. (2) The voltage risetime produced by the Marx generator was short, i.e., $\sim$1 μs. (3) The Marx generator produced a very large electric field at the high-voltage rod, which was certainly greater than the electric field necessary to initiate a spark in the gap.

[9] For the first point, although the large current generated by the Marx generator could conceivably affect the X-ray pulse that was occasionally seen with the negative discharges during the voltage collapse in the gap, most of the X-ray emission was observed to occur near the time the voltage was at a maximum, so it is not obvious how this feature of the Marx generator would come into play. The second point and the third point are related. For the Marx generator used by *Dwyer et al.* [2005a], 15 capacitors, each charged in parallel to 100 kV, are rapidly switched to a series configuration via a sequence of sparks in small gaps within the generator. This causes the potential of the HV electrode in the main gap to rapidly increase. If the potential of the electrode rises faster than the gap can yield to electrical breakdown, then a very large electric field could be produced near the rod electrode. It is conceivable that a similar phenomenon occurs during the leader step formation phase of lightning. Because only a rod-to-ground-plane geometry was used for these experiments, it was not clear if the production of X rays was related to the details of the electrode geometry or if it was due to processes within the air gap. Furthermore, because only 14 long sparks were observed, a more detailed study was desirable.

[10] Recently, *Rahman et al.* [2008] used barium fluoride scintillation detectors, which have a very fast ($\sim$1 ns) response time, to observe X-ray emission from a 1 MV Marx generator, confirming the X-ray observations by *Dwyer et al.* [2005a]. They measured deposited energies from about 30 keV up to a few MeV and found that the X rays arrived in two short bursts, one near the time of the peak voltage and one during the time that the voltage collapsed in the gap.

[11] In this paper, we report the results of a detailed follow-up investigation that is based upon 231 sparks produced by a 1 MV Marx generator, which was previously used by *Rahman et al.* [2008] for studying X-ray production by sparks. We will show that nearly all the original results of *Dwyer et al.* [2005a] are confirmed with these new experiments using different instruments and a different Marx generator and that several new features of the X-ray emission from laboratory sparks are observed, including the observations that very large electric field magnitudes at the electrodes are not necessary to produce X-ray emission in the spark gap. These results shed light not only on how laboratory sparks generate X rays, but also on how X rays are produced by lightning.

2. Experimental Setup

[12] The experiments reported here were performed over a period of three weeks during Spring 2007, at the High-Voltage Laboratory at Uppsala University, Sweden, using a Marx impulse voltage generator (Haefely Test AG, SGSA 1000–50, maximum charging voltage: 1 MV, maximum energy: 50 kJ), capable of producing both negative (HV electrode negative) to ground and positive (HV electrode positive) to ground discharges. In this paper we shall report on experiments using a standard lightning impulse voltage (1.2/50 impulse; front time: 1.2 μs, time to half-value: 50 μs). For some experiments, the generator was reconfigured to deliver a much longer risetime ($\sim$100 μs) switching surge waveform. The X-ray observations from these switching surge experiments will be reported in a separate paper. For most of the present experiments, the gap length was approximately 85 cm, although other lengths were studied. In addition to measuring X rays, we recorded the voltage across the gap and the current flowing to the ground electrode. A capacitive impulse voltage divider (Haefely CS 1000–670) was used to measure the voltage across the gap. The current was measured at the grounded electrode using a current transformer (Pearson model 411, maximum peak current 5 kA, risetime 20 ns, bandwidth 20 MHz).

[13] The basic configuration of the experiment is shown in Figure 2. The X rays were measured by three instruments that were temporarily removed from the Thunderstorm Energetic Radiation Array (TERA) located at the International Center for Lightning Research and Testing (ICLRT) at Camp Blanding, Florida. These instruments have a history of successfully measuring X-ray emission in the electromagnetically noisy environment near both rocket-triggered lightning and natural cloud-to-ground lightning [*Dwyer et al.*, 2005b]. Each instrument contains two detectors: Instruments 1 and 2 each contain two 7.6 cm $\times$ 7.6 cm cylindrical NaI(Tl)/Photomultiplier tube (PMT) detectors (see Figure 3). Instrument 3 contains one NaI(Tl)/PMT

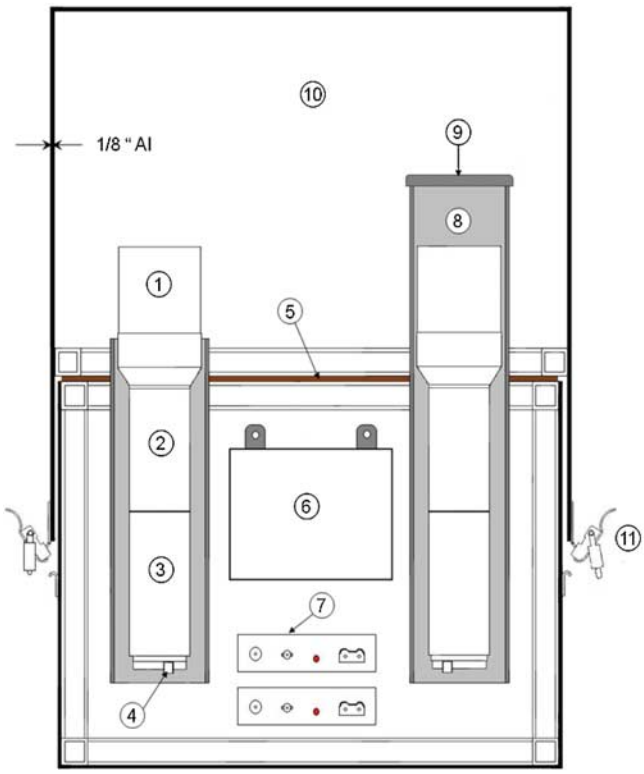

Figure 3. Schematic diagram of one of the three X-ray instruments with attenuated and unattenuated detectors. The components are as follows: (1) 7.6 cm by 7.6 cm NaI scintillator; (2) Photomultiplier tube (PMT) detector; (3) PMT base (HV supply and voltage divider); (4) PMT anode output, which connects directly to the fiber optic transmitter; (5) RF gasket; (6) 12 V battery; (7) FM fiber optic transmitters; (8) lead attenuator (also used as a collimator when the lead cap is removed); (9) lead cap; (10) 0.32 cm thick aluminum box; and (11) latches.

detector and one plastic scintillator (36 cm $\times$ 25 cm $\times$ 1 cm), the latter having a faster time response than the NaI scintillators. The NaI detectors were manufactured by Saint Gobain (3M3 series). The NaI scintillators were mounted to the PMTs and placed inside light-tight aluminum housings with μ-metal shields. The NaI/PMTs were then mounted on Ortec photomultiplier tube bases (model 296), which contained internal HV supplies and divider chains. In addition, the NaI/PMT detectors, which are designed to be light-tight, were wrapped in black electrical tape and in aluminum tape and were checked for light leaks with a bright strobe light before placing the detectors inside the 0.32-cm-thick aluminum boxes. The plastic scintillator/PMT detector was manufactured by mounting a 5.08-cm-diameter PMT to a light guide attached to the end of the scintillator. The assembly was then made light tight by wrapping it in black plastic.

[14] The aluminum boxes and their lids were both welded on eight seams. The lids slid over the bottom of the boxes like a shoe box with a 15-cm overlap between the top and the bottom. The lids were secured tightly with four strong latches that compressed an RF gasket made of copper braid. The inside of the boxes were painted black to absorb any light that might enter through the gaskets. The instruments were powered by internal 12-V batteries. Opticomm FM, analog fiber optic links were used to transmit the signals from the PMT anodes directly to the data acquisition system located in a separate, shielded room. As a result, the detectors were very well shielded from RF noise and light leaks. The aluminum box lids allowed X rays with energies down to about 30 keV to enter from all directions.

[15] Two of the NaI detectors were mounted inside 0.32-cm-thick lead tubes that extended 4.5 cm above the top of the scintillators. The lead also extended 41 cm below the scintillator, completely covering the PMT and the base. When a 0.32-cm-thick lead cap was placed on top of the lead tubes, the overall lead shield served as an attenuator. X-ray energies could be estimated from a comparison of signals from the unattenuated and the attenuated detectors. When the lead cap was removed, the lead tubes could be used as collimators, giving information on the directionality of the X rays. The collimators are effective for X-ray energies below about 300 keV, above which the lead becomes transparent to the X rays. Monte Carlo simulations showed that the collimators restricted the field of view to a 20 degrees cone (half angle). Specifically, X rays incident from a direction 20 degrees off-axis would deposit one half the energy in the collimated detectors compared with the uncollimated detectors.

[16] It was observed that the X-ray emission from the long sparks usually arrives in very fast bursts. Consequently, the total deposited energy measured by a detector is the sum of many X rays and so does not directly give the energy of individual photons. For example, as will be discussed below, many tens of MeV were often measured in a single fast burst lasting only a fraction of a microsecond, and yet the average X-ray energy was typically less than 230 keV. In other words, a single pulse was measured that lasted less than the response time of the detector, and while the equivalent energy was many tens of MeV, it is presumed that it consisted of the superposition of numerous smaller energy deposits from X rays with an average energy less than $\sim$230 keV. By comparing the signals from the unattenuated detectors and the attenuated detectors, it was possible to obtain a rough estimate of the energies involved. A second way to estimate the average X-ray energy, which will also be discussed below, is to observe the Poisson (counting) fluctuations on the unattenuated detectors.

[17] Signals from all six detectors plus a measurement of the electrical current were recorded simultaneously by a Yokogawa 750 ScopeCorder, with 12 bit resolution and a sampling rate of 10 megasamples per second. The scope was usually trigged by the current pulse, and data were recorded for a length of 2 ms with 1 ms of pretrigger sampling. Two channels from Instrument 3 were split off and were recorded along with the current in a Lecroy Wavepro 7100A that sampled at 250 megasamples per second with 8 bit resolution, with a total record length of 1 ms and 0.5 ms of pretrigger sampling. In addition, voltages and current were recorded separately with an 8 ns time resolution.

[18] We note that no control (PMT without a scintillator) detector was used in the present experiments. Control detectors were previously used for the Marx generator experiments described by *Dwyer et al.* [2005a] and for

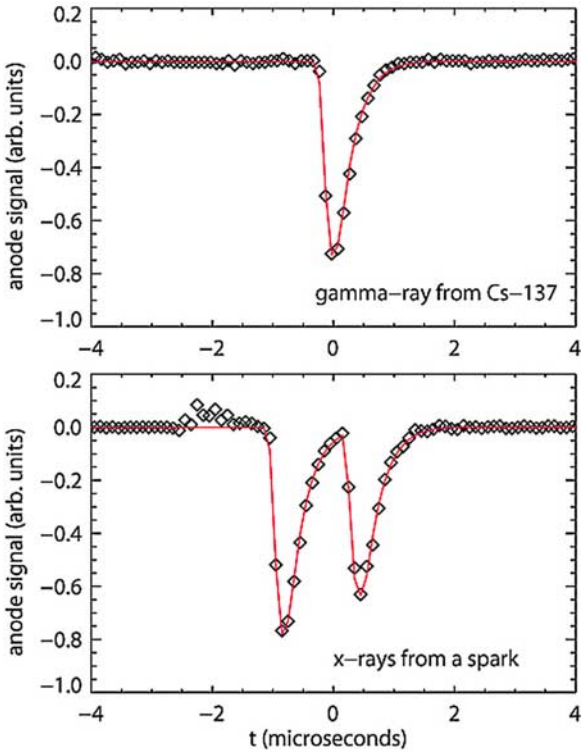

Figure 4. Close-up of X-ray signals during an 85-cm-long, negative 1-MV laboratory spark in air. (top) Measurement of one 662 keV gamma-ray from a Cs-137 radioactive source placed temporarily on top of the detector along with the detector response function. The scales on the two plots are arbitrary and are different from each other. Note that the characteristic NaI decay time is clearly seen in the response. (bottom) X ray from a laboratory spark along with the detector response. The X-ray signals can easily be distinguished from noise due to the characteristic response of the detector.

most of the triggered lightning and natural lightning experiments at the ICLRT during the last 5 years. For all the X-ray observations of lightning and laboratory sparks, involving hundreds of measurements, no significant signal that might be confused with an X-ray measurement has ever been recorded on a control detector. Because the existence of X-ray emission from lightning and laboratory sparks is now well established, and because the performance of the instruments is well known, a control detector was no longer deemed necessary, so that channel was replaced with an active detector.

3. Observations

3.1. Overview

[19] Experiments were performed with several different electrode configurations: The HV and the ground electrodes were either both spheres (2–12 cm in diameter), a rod and sphere, or a rod and plane. The rod was made of brass and had a diameter of 1.0 cm. The tip of the rod was threaded with a diameter of 0.6 cm. The small spherical electrodes were copper with tungsten coating. The larger electrodes were copper with chromium coating. For the negative polarity sparks, some amount of X-ray emission was observed for each electrode configuration. However, the most intense bursts of X rays were observed when two 12-cm-diameter spherical electrodes separated by an 85-cm gap were used.

[20] Figure 4 shows a close-up of X-ray pulses from a negative polarity laboratory spark with a horizontal 85-cm gap and using two 12-cm-diameter spherical electrodes. Figure 4 shows the X-ray signals from the PMT anode (diamonds) along with the detector response function (red). In Figure 4 (bottom), two distinct X-ray pulses can be seen. For comparison, the measurement of a single 662-keV gamma ray from a Cs-137 radioactive source, placed temporarily on top of the detector, is shown (top). Note that the scales on the two plots are arbitrary and are different from each other. Figure 5 shows the X-ray pulses from another negative spark with the same configuration, along with the current and voltage waveforms. The current is measured through the grounding cable connected to the grounded electrode, and so a negative polarity spark will result in a positive current pulse and vice versa. Figure 6 shows an example of a positive polarity spark (horizontal 85-cm gap with a positive 12-cm-diameter spherical electrode and a grounded rod).

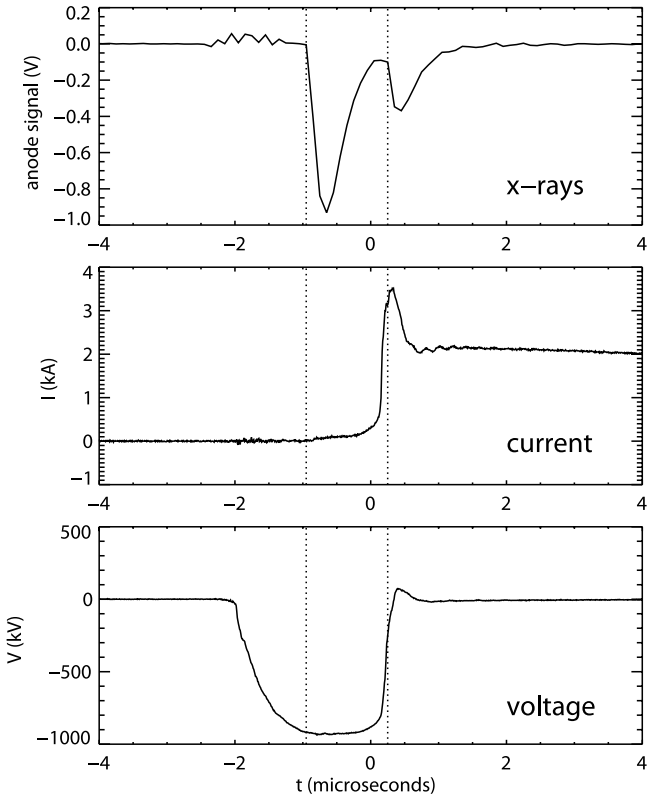

Figure 5. X-ray emission from an 85-cm-long, negative 1-MV laboratory spark in air at standard pressure. (top) X-ray signal from the anode of the NaI/PMT detector. (middle) Current through the gap. (bottom) Gap voltage. As can be seen, there are two distinct pulses of X rays, one occurring near the time that the voltage is at a maximum and one near the time when the current is at maximum, when the voltage in the gap is collapsing.

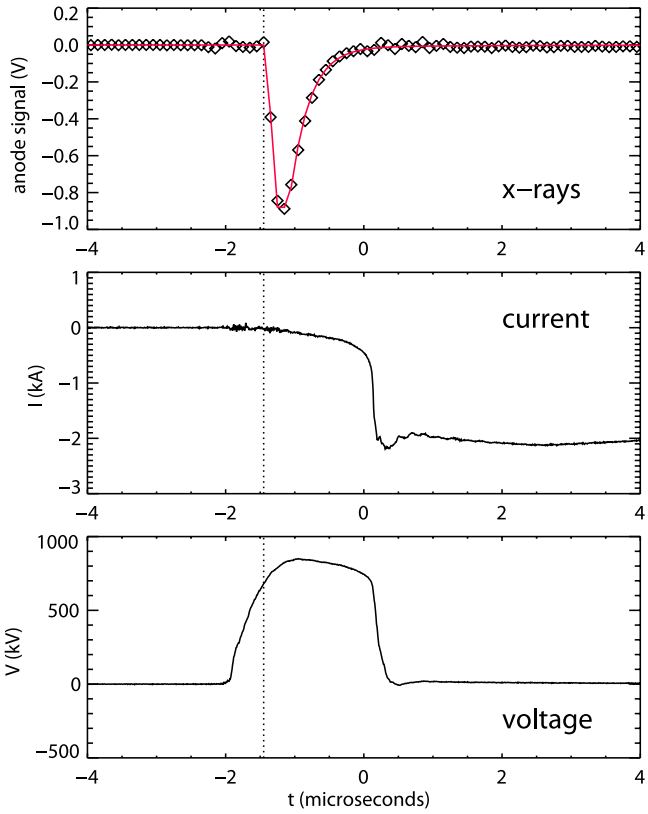

Figure 6. X-ray emission from an 85-cm-long, positive 1-MV laboratory spark in air at standard pressure. (top) X-ray signal from the anode of the NaI/PMT detector. (middle) Current through the gap. (bottom) Gap voltage.

[21] The X-ray pulses observed during these experiments were relatively large signals taken directly from the PMT anode. They were easily distinguished from electromagnetic noise because of the characteristic response of the detectors. Specifically, the pulse risetime is due to the NaI scintillation decay time and the pulse fall time is due to the front-end shaping electronics. Also, false signals due to optical emission could be ruled out, since the X-ray signals did not follow the bright optical emission associated with the arc. The background counts in the detectors were typically about 100 counts/second and so the probability that even a single count occurred within 4 μs of the spark (as in Figures 4–6) is extremely small, thus, random coincidences with naturally occurring background could be completely excluded. This can be easily seen in Figure 7, which shows a typical data record with a longer time window. The large pulse in the center is due to the X rays associated with the spark. No other pulses due to background are present.

[22] For the first 88 (positive and negative) sparks, the spark gap was vertical with the HV electrode suspended above the grounded electrode. In all of these vertical sparks in which X rays were detected, the X rays were detected as a very fast burst that occurred when the current in the gap was largest and when the voltage in the gap was nearly collapsed.

[23] Starting at spark 89, the spark gap geometry was changed to horizontal, with both electrodes being about 140 cm above the ground. In this configuration, X rays were observed to arrive in a very short burst at about the time that the voltage across the gap was reaching its maximum value, about 1 μs before the gap voltage started to collapse and the large current pulse began. This X-ray pulse is henceforth referred to as the first X-ray pulse. In many cases the second X-ray pulse, similar to that described for the vertical geometry above, still occurred during the voltage collapse. Henceforth, that pulse is referred to as the second X-ray pulse. The observations of these first and second X-ray pulses agree with the results of *Rahman et al.* [2008], who reported similar pulses. In addition, when 12-cm-diameter spherical electrodes were used in the horizontal configuration, the intensity of the detected X rays in the first pulse increased noticeably.

[24] A summary of the basic results of the experiments, with different electrode geometries and configurations, is given in Table 1. As discussed above, each configuration used an assortment of different electrode diameters. However, the 12-cm-diameter electrodes, which produced the brightest X-ray pulses, were used only for the horizontal configuration, which may explain the larger occurrence of the first pulse for the horizontal configuration. The threshold for the detection of X rays during these experiments was 100 keV in a single detector. In Table 1, X rays are detected if an X-ray pulse, >100 keV, is measured by at least one of the three unattenuated detectors. This >100 keV X-ray pulse could come from either an individual X ray or from the simultaneous detection of several lower energy X rays. Note that the X rays must have energies greater than about 30 keV in order to penetrate the aluminum lids.

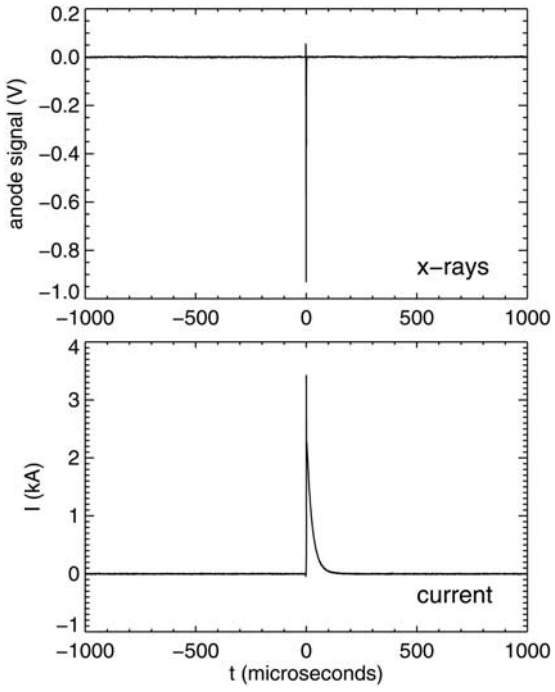

Figure 7. X-ray signals and current during an 85-cm-long, negative 1-MV laboratory spark in air with an expanded time window to show the low background level (same spark as in Figures 5). The time that the spark occurred (current peak) is at $t = 0$ in the plot.

Table 1. Summary of X-ray Observations

Polarity	Electrode Configuration	Number of Sparks	Occurrence of First X-ray Pulses, %	Occurrence of Second X-ray Pulses, %
negative	vertical	82	0	60
negative	horizontal	121	37	64
positive	vertical	6	0	0
positive	horizontal	22	14	0

[25] Overall, X rays in either the first or second pulses were observed in 68% of the 203 negative polarity sparks and X rays (first pulse only) were observed in 11% of the 28 positive polarity sparks. The average deposited energy in the three unattenuated NaI detectors for the negative polarity sparks was 9.0 MeV for the first X-ray pulse and 5.2 MeV for the second pulse. The average deposited energy in the three unattenuated NaI detectors for the positive polarity sparks was 2 MeV. One factor that may have biased the positive polarity results is that the breakdown voltage for positive polarity was lower than for negative polarity.

[26] The spectra of the total deposited energy in the three unattenuated detectors for the negative polarity sparks (first and second pulses) and the positive polarity sparks is shown in Figure 8. Figure 8 shows the distribution of brightness of the sparks as they appear in X rays. It should be emphasized that these spectra are not the same as the energy spectra of individual X rays, since many X rays are detected at the same time. As can be seen, the first X-ray pulse for negative sparks extends to much higher energies than the other cases. Interestingly, the second pulse for negative sparks appears to peak around 2–3 MeV. The fact that all three spectra have different shapes, i.e., different brightness distributions, may imply that more than one mechanism is involved in the production of X rays.

3.2. Source Locations Estimated Using Collimated Detectors

[27] The occurrence times of the X rays in the second pulses were not what one would expect if large electric fields in the gap were producing the runaway electrons. When collimated detectors were used to view the gap from various directions, it was found that for the second pulse no significant numbers of X rays were being emitted from the gap, the Marx generator, or the voltage divider. Instead, the X rays appeared to be coming from the space above the instruments, the Marx generator, voltage divider, and the gap.

[28] The intensity of the first X-ray pulses appears to be sensitive to the size and configuration of the electrodes, whereas the second pulse does not seem to depend very much upon the electrode and gap geometries. Conversely, the intensity of the second pulse depends upon the arrangement of the HV components away from the gap, specifically the presence of the HV capacitive divider. These facts provide evidence that the first and second pulses are produced at different locations.

[29] Collimated detectors confirmed that the first X-ray pulse, unlike the second, did indeed originate from the gap. When the gap was viewed by the collimated detector, the deposited energy in the collimated detector was found to be 50% that of the uncollimated detector in the same box. In contrast, when a collimated detector looked away from the gap toward the ceiling, the deposited energy in the collimated detector was found to be less than 4% of the uncollimated detector. This number is close to the 3% found when the lead cap was placed on the collimator, suggesting that in this case most of the X rays observed by the collimated detector were high-energy X rays penetrating the sides of the collimator and not originating away from the gap. The fact that when the collimators, which had a wide field of view, looked at the gap, they detected only 50% of the X-ray energy seen by the uncollimated detector, suggests that the source of the X rays from the gap may be diffuse and not just located at the anode. For example, using the dependence of the effective area versus angle along with the distance from the detectors to the gap suggests a source diameter of roughly 1 m. However, other effects such as Compton scattering of the X rays from objects in the room and within the instruments may also be important, so further experimental work and modeling, including more Monte Carlo simulations, is needed before firm conclusions about the source region can be made.

3.3. Energy Spectra Obtained Using Attenuated Detectors

[30] In most cases, no X-ray signals were observed by the attenuated detectors despite large intensities of X rays being observed on all of the un-attenuated detectors. However, in 15 of the negative polarity sparks, X-ray signals above 100 keV were detected by the attenuated detectors for the first pulse. One such signal is shown in Figure 9. Note that the unattenuated detector is badly saturated in this case. However, using the signals from the "fast" plastic scintillator to extract the X-ray time profile, we can find the deposited energy in the unattenuated detector by fitting the response function to the unsaturated parts of the signal. We believe that this method produces reliable energies on the basis of tests with cosmic ray muons, which produce a similar level of saturation. The deposited energies in this spark are found to be 1.5 MeV for the attenuated detector and 38 MeV for the first pulse in the unattenuated detector.

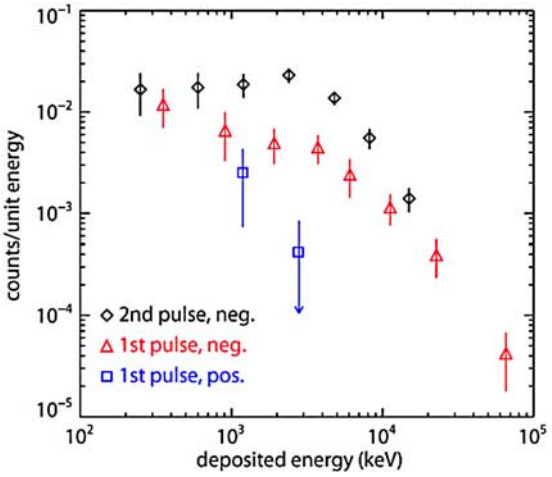

Figure 8. Spectra of total deposited energy in the three unattenuated detectors versus energy.

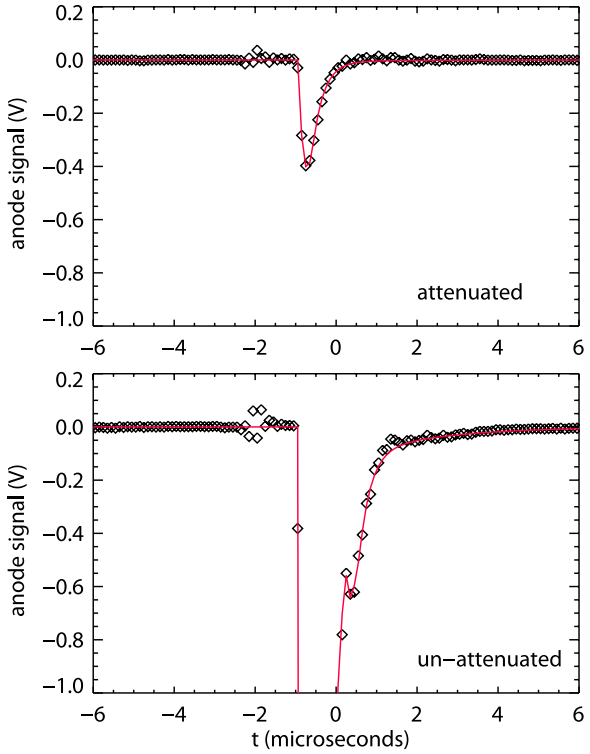

Figure 9. X-ray signals from the attenuated and unattenuated detectors for a negative sparks.

Figure 10 shows the attenuated detector signal versus the un-attenuated detector signal, for two detectors in the same box, for the first pulse for all the sparks. The cluster of points near 270 keV has a natural interpretation illustrated in Figure 11, which shows the detection efficiency of the NaI detectors covered by a 0.32-cm-thick lead attenuator. Specifically, the curve in Figure 11 (top), which was calculated by a detailed Monte Carlo simulation, is the ratio of the number of detected photons to the number of incident photons versus incident photon energy. Also shown in

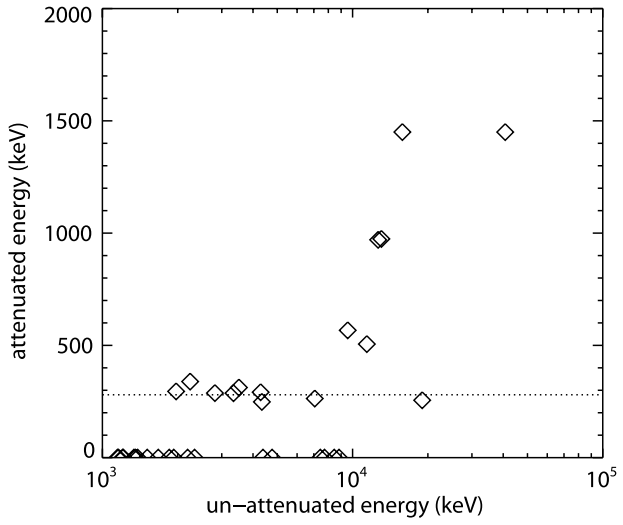

Figure 10. Deposited energy for an attenuated detector versus deposited energy for the unattenuated detector in the same box.

Figure 11 (top) is the expected energy spectrum produced by bremsstrahlung radiation for an electron beam initially at 400 keV and allowed to lose energy through ionization processes. Since the true energy spectrum of electrons is not known, a monoenergetic initial energy is used in order to illustrate some properties of the X-ray emission. Figure 11 (bottom) shows the resulting number of detected photons versus deposited energy calculated by the Monte Carlo simulation. As can be seen, there is a clustering of photons around 270 keV, with a few below about 200 keV, which agrees well with the observations. Because the data points above 300 keV in the attenuated detector, seen on Figure 10 (left), cannot result from the sum of two lower energy X rays (they would not penetrate the lead), this suggests that X rays with energies of 300 keV or higher are sometimes present. This also implies that electrons with energies above 300 keV must also be present in order to produce such energetic X rays.

[31] For more intense events, corresponding to the data on the right hand side of Figure 10, the signal measured by the attenuated detector will be composed of many photons distributed as shown in Figure 11. In this case, the total deposited energy will be much larger than 270 keV, since many photons are detected at the same time. As a result, an X ray and hence the electron spectrum extending up to about 400 keV, but not much above 400 keV, is consistent with the data. This energy is similar to the energies inferred by *Dwyer et al.* [2004a] from triggered lightning leaders.

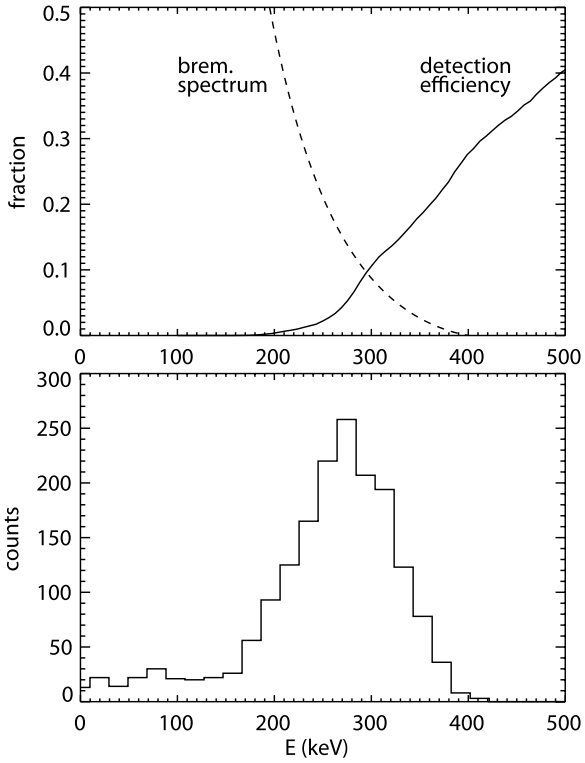

Figure 11. (top) Attenuated detector efficiency versus X-ray energy and energy spectrum due to bremsstrahlung emission from 400-keV electrons in air. (bottom) Monte Carlo simulation of the deposited energy distribution in the attenuated detector for the input X-ray spectrum shown in the top plot.

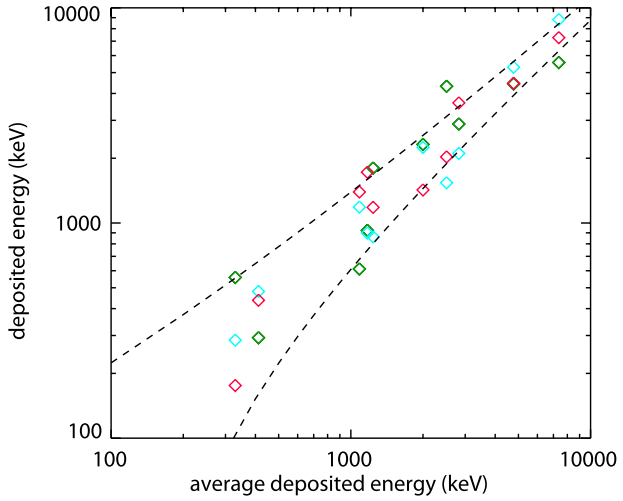

Figure 12. Signals from the three unattenuated NaI detectors for a negative spark. Each color corresponds to a different detector. The small Poisson fluctuations seen in this and other sparks are used to infer an upper limit on the average X-ray energy of 230 keV. The dashed lines show the 1-sigma range expected for fluctuations for this average X-ray energy.

This number is also a substantial fraction of the maximum kinetic energy that the electrons can gain from an electrostatic electric field, for example, the maximum voltage for negative sparks was typically 930 kV for an 85-cm gap. Note that it is unlikely that the detectors are measuring the energetic electrons directly, since a minimum ionizing electron would lose at least 1 MeV in passing though the aluminum lid. Also, the plastic scintillator, which should be more sensitive to electrons than X rays, generally, saw very small signals, consistent with X rays.

3.4. Average X-ray Energy Estimated Using Poisson Fluctuations

[32] The X-ray emission is often seen to have approximately the same intensity on all three un-attenuated detectors whenever they are placed at the same distance from the source and approximately on the same side of the gap. In experiments in which the electrodes were arranged horizontally and X-ray emission was measured from both ends of the gap, the X-ray emission for negative discharges was found to be a factor of 3.4 larger behind the ground electrode, consistent with the runaway electrons being accelerated by the electric field within the gap itself. Substantial emission in this case is also observed to the sides, indicating that the X rays are emitted with a broad angular distribution. In addition, on the basis of the physics of bremsstrahlung emission, the expected emission half-angle varies approximately as $1/\gamma$, where γ is the Lorentz factor of the runaway electrons. If we take 400 keV as a maximum energy (see above), then the resultant beam will have a half angle of roughly 30 degrees. In reality, the electrons will have a wide range of energies below 400 keV and may themselves have a broad angular distribution, both due to elastic scattering and due to the electric field pattern. As a result, 30 degrees is a conservative lower bound for the half angle of the X-ray emission. Given that the X rays appear to be emitted with a broad angular distribution, a comparison of the total deposited energies in the unattenuated (and uncollimated) detectors can be used to estimate the average energy of the X rays using the observed Poisson fluctuations (counting statistics). This approach is illustrated in Figure 12, which shows the outputs of three unattenuated detectors for a subset of the sparks in which the three detectors were within 90 degrees of each other from the spark axis. Figure 12 shows the detected energies from the individual unattenuated/uncollimated detectors versus the average detected energy in all three detectors for the first X-ray pulses. It is found, when assuming that all the variation between detectors was due to Poisson fluctuations, that an average photon energy of 230 keV was required. The dashed lines show the expected ±1 sigma values based upon an average photon energy of 230 keV. The dashed lines take into account the correlation between x and y axes, which reduces the degrees of freedom by 1. Because both systematic differences in the detectors and statistical variations (other than counting statistics) will likely affect the scatter in the data points, including these variations as if they were due to Poisson fluctuations will result in an underestimate in the number of detected photons and an overestimate in the average photon energy. As a result, 230 keV should be taken as an upper limit in the average X-ray energy for emission from the spark gap, consistent with the results based upon the lead attenuators.

3.5. X-ray Pulse Durations

[33] During some of the larger X-ray pulses, the signal measured by the "fast" plastic scintillator was large enough to make detailed measurements of the pulse duration. This X-ray signal is shown in Figure 13, along with the detector response. As can be seen, the width of the X-ray pulse is consistent with the detector response for a single particle (Figure 13, top). By comparing the detector response with the data, it is found that the duration of the X rays that created the pulse in this case is less than 8 ns. Because this event was very bright in X rays, it is likely that, as with the NaI detectors, this signal is composed of many detected X rays. With this assumption, the lifetime of the X-ray source must also be less than 8 ns.

[34] One possible location of the runaway electron source is the streamer tips in the gap. Streamers are propagating discharges that do not involve substantial heating of the air. If one assumes a typical streamer speed of 10^7 m/s, the 8-ns duration implies that the runaway electrons, if produced at the streamer tips, were produced over a streamer propagation distance of no more than 8 cm. This is smaller than the gap length but comparable in size to the spherical electrode, where the electric fields are the largest.

[35] In 2 out of 14 sparks observed by the fast plastic scintillator, the first pulse seen by the NaI detectors was found to be composed of two separate pulses (not to be confused with the "first" and "second" X-ray pulses, the latter one occurring at the time of the voltage collapse). The time interval between these pulses is 150 ns on average. Figure 14 shows an example of these two pulses.

3.6. Varying Gap Lengths

[36] Experiments were performed varying the gap length and the breakdown voltage. These two parameters are

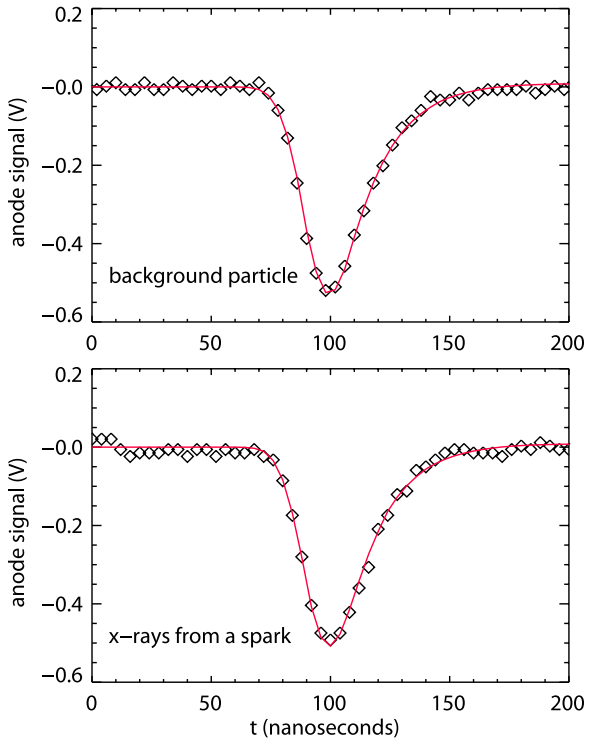

Figure 13. X-ray signals from the "fast" plastic scintillation detector during a negative 1-MV laboratory spark in air with the detector response. (top) Response due to a single background energetic charged particle, presumably a relativistic cosmic ray secondary muon or electron. The empirical detector response function is also shown (smooth curve). (bottom) X rays from a spark with the same response function.

necessarily related, since longer gaps require higher voltage to breakdown for a fixed voltage risetime. It was found that as the gap lengths and the voltages were reduced the intensity of the X rays also decreased. X rays were observed with gap lengths as short as 20 cm with voltages as low as 472 kV. For 10-cm gaps, no X rays were observed. Thus, even relatively small sparks can produce X rays, lending support to the observations by *Dwyer et al.* [2005a] that the small gaps within the Marx generator were also generating X rays.

4. Discussion

[37] As discussed in the last section, the first X-ray pulse occurred when the voltage across the gap was at or near a maximum value, whereas the second pulse occurred when the voltage in the gap nearly collapsed and the current was near maximum. However, at this latter time in the discharge, the electric field near some HV components in the circuit might have been large owing to the grounding of the conductors in the presence of previously produced space charge, as discussed in more detail in the next paragraph. Along with the results of the collimated detectors, these facts suggest that the first X-ray pulses were due to processes within the spark gap and the second pulses were due to processes that occurred outside the gap, perhaps near other HV components in the circuit during the primary current flow.

[38] The second X-ray pulse, occurring during the voltage collapse, was difficult to study since the exact location(s) of the source were not known. Its presence and characteristics depended upon the details of the HV setup. When the capacitive voltage divider was removed, the second pulse disappeared. However, using the collimated detectors, it was found that X rays were not coming from the divider itself. In addition, although some X rays seemed to be originating from the space immediately above the divider, X rays seemed to be coming from other directions overhead as well. The second pulse was never seen for positive sparks, indicating that the polarity or breakdown voltage may be important. One possible scenario is that while the Marx generator fires and subjects the HV electrode and wiring to the full 1-MV potential, corona (space charge) is generated, reducing the electric field around the HV components. When the gap breaks down and the voltage rapidly collapses, the HV components are grounded. These components then find themselves at nearly zero (ground) potential relative to the space charge produced when 1 MV was present. This space charge necessarily produces a large electric field in the opposite direction, potentially resulting in streamers being emitted to neutralize the space charge [*Cabrera and Cooray*, 1992]. It is possible that X rays are being emitted during this burst of streamers. The importance of the capacitive divider may either be that its HV conductors are emitting the streamers or its large capacitance is playing some role in the process. If this mechanism is what is producing the X rays then a similar process may be occurring during lightning leaders and return strokes, for which the rapid change in potential in the highly conducting channel core leads to streamer development to remove charge from the corona sheath [e.g., *Maslowski and Rakov*, 2006]. *Dwyer et al.* [2003, 2004a] found some evidence that the return stroke could also be a source of X rays, and so this possibility should be investigated further.

[39] One puzzling aspect of these experiments is why the first X-ray pulse in the gap was not observed for the first

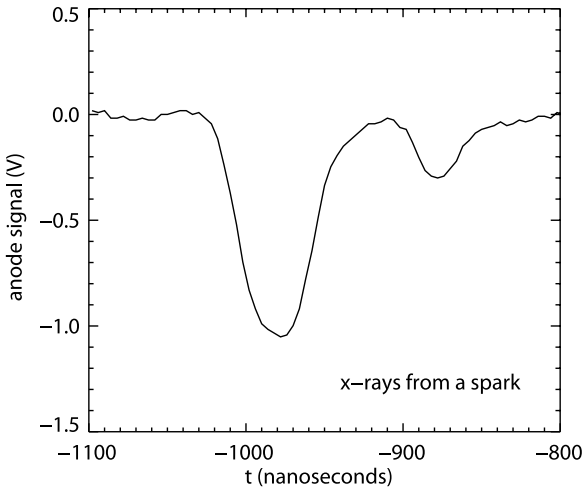

Figure 14. X-ray signals from the fast plastic scintillation detector during a negative 1-MV laboratory spark in air, showing two distinct pulses.

88 sparks, when the gap and spark were vertical. For horizontal gaps, it was found that a substantial amount of X-ray energy could be observed at large angles, even behind the cathode, so X rays should have been observable for the vertical gap even though the beam was predominantly directed toward the ground. Even for the horizontal case, when relatively large numbers of X rays were observed from the gap, a significant fraction of the sparks did not result in any observable X rays although the general conditions appeared to be similar.

[40] The fact that the larger electrodes produced the most X rays in the gap (at least for the negative sparks) suggests that it is not the electric field configuration at the HV electrode that is producing the runaway electrons. For example, the local electric field near a rod is much larger than near the surface of a 12-cm sphere, and yet the sphere resulted in more X rays. Therefore, these experiments provide evidence that for negative sparks the runaway electrons are generated by processes within the gap and not by processes at the electrodes. (Of course, if the runaway electrons strike the anode and the anode is a high-Z material then X-ray emission could be enhanced.) The process that results in the runaway electron production could be either the leader channel that is in the process of traversing the gap or the streamers in the gap. In addition, as the streamers approach the opposite electrode or streamers of opposite polarity then the electric field could be enhanced above that which normally occurs near the streamer tips. One possible reason that the larger diameter electrodes make more intense X rays than smaller electrodes is that larger electrodes can generate a higher voltage in the gap before breakdown occurs.

[41] The polarity asymmetry in the production of X rays as reported above is quite dramatic. This asymmetry occurs even when identically shaped electrodes are used. However, even though the electrode geometry is symmetrical, the overall configurations for cases when the HV electrode is positive and the HV electrode is negative are not necessarily the same, owing to the capacitance between the electrodes and the surrounding room features. For example, the floor below the detectors and the spark gap is a grounded metal plane. The result will be a larger electric field at the surface of the HV electrode than at the grounded electrode. In addition, positive and negative streamers and positive and negative leaders have distinctly different properties, which may lead to the asymmetry seen in the X-ray emission.

[42] It is not clear how the first and second X-ray pulses reported in this paper are related to the X rays from lightning [*Dwyer et al.*, 2005b]. Moreover, it is not clear how the individual X-ray pulses seen in Figure 14 with the plastic scintillator relate to the X-ray pulses produced by lightning. For example, because X-ray pulses are observed to be associated with the step formation process in lightning, are the pulses produced by the laboratory sparks also associated with some kind of leader stepping? Or, conversely, do lightning X-ray pulses have a finer time structure variation, similar to that seen for sparks?

5. Summary

[43] The experiments described in the paper verify several of the salient results of *Dwyer et al.* [2005a] and present some new results. These findings are summarized as follows. (1) X rays with energies above ~30 keV (the measurement minimum) are produced by long laboratory sparks in air at atmospheric pressure. (2) X rays are produced by both negative and positive polarity sparks, where the polarity is defined by the polarity of the HV electrode. (3) X rays are produced in gap lengths as short as 20 cm with voltages as low as about 500 kV. (4) X-ray pulses often occur near or slightly before the time when voltage across the gap attains its maximum. (5) A second distinct X-ray pulse often occurs when the voltage across the gap is collapsing and when the current through the gap is near its maximum. This second pulse appears to originate from above the gap. (6) The average energy of the X-ray photons less than 230 keV is found to be consistent with the observations, but occasionally X rays with energies in excess of 300 keV were detected.

[44] Because the X-ray emission from laboratory sparks shows many similarities to the emission observed from natural and rocket-triggered lightning, they may share a common production mechanism, although further detailed investigation of both laboratory sparks and lightning is needed to clarify these similarities. Because X-ray emission is a common property of both stepped and dart leaders, understanding this emission may shed light on the basic properties of how lightning leaders propagate. Laboratory sparks are more easily studied than lightning and so these X-ray measurements may provide new insight into lightning processes and their relationship to laboratory sparks. On the other hand, laboratory sparks are also complex and much work still remains in order to understand their detailed physics. Investigating the X-ray emission from laboratory sparks may provide additional insight into sparks, allowing new theoretical work and new experimental tests. In particular, because the production of runaway electrons should be sensitive to the electric field strengths in the source region, measuring the X rays produced by runaway electrons may help determine the electric fields during conditions that would be very difficult the measure otherwise.

[45] **Acknowledgments.** We would like to thank Marcus Hohlmann for his assistance with the plastic scintillation detectors. This work was supported by the NSF grants ATM 0607885, ATM 0420820, and ATM 0346164 and NSF CAREER grant ATM 0133773. The participation of the Uppsala group in the research project was funded by grants from the Swedish Foundation for International Cooperation in Research and Higher Education (STINT), grant IG2004–2031, and Swedish Research Council, grant 621-2006-4299.

References

Babich, L. P., T. V. Loiko, L. V. Tarasova, and V. A. Tsukerman (1975), Nature of X rays and fast electrons from nanosecond gas discharges, *Sov. Tech. Phys. Lett.*, *1*(2), 79–80.

Brown, S. C. (1966), *Introduction to Electrical Discharges in Gases*, 190 pp., John Wiley, Hoboken, N. J.

Cabrera, V. M., and V. Cooray (1992), On the mechanism of space charge generation and neutralization in a coaxial cylindrical configuration in air, *J. Electrost.*, *28*, 187–196, doi:10.1016/0304-3886(92)90070-A.

Coleman, L. M., and J. R. Dwyer (2006), The Propagation speed of runaway electron avalanches, *Geophys. Res. Lett.*, *33*, L11810, doi:10.1029/2006GL025863.

Dwyer, J. R. (2003), A fundamental limit on electric fields in air, *Geophys. Res. Lett.*, *30*(20), 2055, doi:10.1029/2003GL017781.

Dwyer, J. R. (2004), Implications of X-ray emission from lightning, *Geophys. Res. Lett.*, *31*, L12102, doi:10.1029/2004GL019795.

Dwyer, J. R. (2007), Relativistic breakdown in planetary atmospheres, *Phys. Plasmas*, *14*(4), 042901, doi:10.1063/1.2709652.

Dwyer, J. R., and D. M. Smith (2005), A comparison between Monte Carlo simulations of runaway breakdown and terrestrial gamma-ray flash observations, *Geophys. Res. Lett.*, *32*, L22804, doi:10.1029/2005GL023848.

Dwyer, J. R., et al. (2003), Energetic radiation produced during rocket-triggered lightning, *Science*, *299*, 694, doi:10.1126/science.1078940.

Dwyer, J. R., et al. (2004a), Measurements of X-ray emission from rocket-triggered lightning, *Geophys. Res. Lett.*, *31*, L05118, doi:10.1029/2003GL018770.

Dwyer, J. R., et al. (2004b), A ground level gamma-ray burst observed in association with rocket-triggered lightning, *Geophys. Res. Lett.*, *31*, L05119, doi:10.1029/2003GL018771.

Dwyer, J. R., H. K. Rassoul, Z. Saleh, M. A. Uman, J. Jerauld, and J. A. Plumer (2005a), X-ray bursts produced by laboratory sparks in air, *Geophys. Res. Lett.*, *32*, L20809, doi:10.1029/2005GL024027.

Dwyer, J. R., et al. (2005b), X-ray bursts associated with leader steps in cloud-to-ground lightning, *Geophys. Res. Lett.*, *32*, L01803, doi:10.1029/2004GL021782.

Fishman, G. J., et al. (1994), Discovery of intense gamma-ray flashes of atmospheric origin, *Science*, *264*, 1313–1316, doi:10.1126/science.264.5163.1313.

Gurevich, A. V. (1961), On the theory of runaway electrons, *Sov. Phys. JETP, Engl. Transl.*, *12*(5), 904–912.

Gurevich, A. V., and K. P. Zybin (2001), Runaway breakdown and electric discharges in thunderstorms, *Phys. Uspekhi*, *44*, 1119, doi:10.1070/PU2001v044n11ABEH000939.

Gurevich, A. V., G. M. Milikh, and R. A. Roussel-Dupré (1992), Runaway electron mechanism of air breakdown and preconditioning during a thunderstorm, *Phys. Lett. A*, *165*, 463, doi:10.1016/0375-9601(92)90348-P.

Lehtinen, N. G., T. F. Bell, and U. S. Inan (1999), Monte Carlo simulation of runaway MeV electron breakdown with application to red sprites and terrestrial gamma ray flashes, *J. Geophys. Res.*, *104*(A11), 24,699–24,712, doi:10.1029/1999JA900335.

Maslowski, G., and V. A. Rakov (2006), A study of the lightning channel corona sheath, *J. Geophys. Res.*, *111*, D14110, doi:10.1029/2005JD006858.

Moore, C. B., K. B. Eack, G. D. Aulich, and W. Rison (2001), Energetic radiation associated with lightning stepped-leaders, *Geophys. Res. Lett.*, *28*, 2141–2144, doi:10.1029/2001GL013140.

Moss, G. D., V. P. Pasko, N. Liu, and G. Veronis (2006), Monte Carlo model for analysis of thermal runaway electrons in streamer tips in transient luminous events and streamer zones of lightning leaders, *J. Geophys. Res.*, *111*, A02307, doi:10.1029/2005JA011350.

Noggle, R. C., E. P. Krider, and J. R. Wayland (1968), A search for X-rays from helium and air discharges at atmospheric pressure, *J. Appl. Phys.*, *39*(10), 4746–4748, doi:10.1063/1.1655832.

Rahman, M., V. Cooray, N. A. Ahmad, J. Nyberg, V. A. Rakov, and S. Sharma (2008), X rays from 80-cm long sparks in air, *Geophys. Res. Lett.*, *35*, L06805, doi:10.1029/2007GL032678.

Smith, D. M., L. I. Lopez, R. P. Lin, and C. P. Barrington-Leigh (2005), Terrestrial gamma-ray flashes observed up to 20 MeV, *Science*, *307*, 1085–1088, doi:10.1126/science.1107466.

Stankevich, Y. L., and V. G. Kalinin (1968), Fast electrons and X-ray radiation during the initial stage of growth of a pulsed spark discharge in air, *Sov. Phys. Dokl., Engl. Transl.*, *12*(11), 1042–1043.

Tarasova, L. V., and L. N. Khudyakova (1970), X rays from pulsed discharges in air, *Sov. Phys. Tech. Phys., Engl. Transl.*, *14*(8), 1148–1150.

Tarasova, L. V., L. N. Khudyakova, T. V. Loiko, and V. A. Tsukerman (1974), Fast electrons and X rays from nanosecond gas discharges at 0.1–760 torr, *Sov. Phys. Tech. Phys., Engl. Transl.*, *19*(3), 351–353.

Va'vra, J., J. A. Maly, and P. M. Va'vra (1998), Soft X-ray production in spark discharges in hydrogen, nitrogen, air, argon and xenon gases, *Nucl. Instrum. Methods*, *418*, 405–419.

Wilson, C. T. R. (1925), The acceleration of beta-particles in strong electric fields such as those of thunder-clouds, *Proc. Cambridge Philos. Soc.*, *22*, 534–538.

D. Concha, J. R. Dwyer, H. K. Rassoul, and Z. Saleh, Department of Physics and Space Sciences, Florida Institute of Technology, Melbourne, FL 32901, USA. (jdwyer@fit.edu)

V. Cooray and M. Rahman, Ångström Laboratory, Division for Electricity and Lightning Research, Department of Engineering Sciences, Uppsala University, Box 534, SE-75121 Uppsala, Sweden.

J. Jerauld, Raytheon Missile Systems, 1151 East Hermans Road, Tucson, AZ 85706, USA.

M. A. Uman and V. A. Rakov, Department of Electrical and Computer Engineering, University of Florida, P.O. Box 116130, Gainesville, FL 32611, USA.